

Gold nanoparticles and emerging applications in imaging

R. Sharma^{*}, A. Sharma^{**}

^{*}Nanotechnology Lab, Electrical Engineering Department, Maharana Pratap A&T University, Udaipur, Rajasthan 313001, India; ^{**}Innovations And Solutions Inc.USA,3945 W Pensacola Street,#98, Tallahassee, Florida 32304 USA

ABSTRACT

Au from Au–Ag core–shell nanoparticles act as multimodal Gold-speckled silica nanoparticles as contrast agents for noninvasive imaging with magnetic resonance imaging, computer tomography and photoacoustic tomography. These Au nanoparticles can be prepared in a simple one-pot synthesis using nonionic microemulsions. These nanoparticles can be made useful for magnetic resonance contrast (provided through gadolinium incorporated in the silica matrix) whereas the photoacoustic signal originates from nonuniform, discontinuous gold nanodomains speckled across the silica surface. Functionalized gold nanoparticles act as contrast agents for both in vivo X-ray and magnetic resonance imaging. These particles are formed by encapsulating gold cores within a multilayered organic shell which is composed of gadolinium chelates bound to each other through disulfide bonds. We observed the magnetic moments as MRI properties showing contrast enhancement in MRI due to presence of gadolinium ions entrapped in the organic shell, whereas the gold core generated a strong X-ray absorption. This combination revealed that these gold nano-nut particles are suited for dual modality imaging and freely circulate in the blood vessels without undesirable accumulation in the lungs, spleen, and liver.

Key words: gold nanoparticles, imaging, CT, X-ray imaging, photoacoustics.

1 INTRODUCTION

Functionalized nanoparticles (NPs) is an emerging art and intensive study is aimed at creating them useful tools for molecular diagnosis, therapy, and biotechnology. Application of magnetic resonance molecular imaging (MRI) suffers from intrinsically low sensitivity because of the physical limitations of the technique. So, goal of high resolution mainly rely on the development of efficient contrast agents. Gadolinium-based agents, the efficiency can be augmented by increasing the relaxation enhancement induced by a single paramagnetic Gd^{3+} ion and by bringing a large number of these ions to the molecular target tissue. From theoretical considerations, a relaxation enhancement (relaxivity) of $\mu 100 \text{ mM}^{-1} \text{ s}^{-1}$ induced by $1 \text{ mM } Gd^{3+}$ can be expected as a maximum for $T1$ contrast agents. However, the number of Gd^{3+} ions that can be delivered to a specific tissue volume element is not restricted by stringent physics rules but by the challenging synthesis of complex

compounds and more soft biological and chemical limitations. This fact motivated the science community to look for new alternatives as a route for creating nano sized units that can be loaded with chelating ligands involving nanocrystals made of noble metals such as gold or silver.

2 GOLD NANOPARTICLES

In following sections, gold NPs and their applications are described. Gold nanoparticles are easily functionalized by thiol derivatives, opening multimodal imaging perspectives. To design a potential MRI contrast agent, nanocrystals coated with Gd^{3+} chelates present the advantage of a generating a rigid core that minimizes internal degrees of freedom. Another interesting aspect is the high electron density of these heavy-metal objects, promising gold NPs as agents for X-ray and CT imaging. Multimodal imaging techniques have emerged using MRI-CT hybrid imaging and gold nanoparticles have unique role to answer for this multimodal art. The technique depends on the fact that gold NPs show intrinsic magnetization of Au in thiol-capped gold NPs with a permanent magnetism at room temperature. With respect to MRI, it is conceivable that the metallic core of an NP coated with gadolinium chelate thiol derivatives can contribute to the relaxivity of the bulk water molecules, in addition to the contribution from the electron spin of the Gd^{3+} ions.

3 THIOL DERIVATIVES AS GOLD NANOPARTICLES

In the present paper, a thiol derivative DTTA13 chelate (called Dt) is focus as the protective agent for the Au NPs. For illustration, batches of gold Dt-coated NPs (DtNP) are shown synthesized using different $HAuCl_4/Dt$ ratios [Table S1 in the Supporting Information (SI)]. DtNPs can be complexed with gadolinium(III) and yttrium(III) by mixing solutions of DtNPs with a slight excess of aqueous solutions of $LnCl_3$ ($Ln = Gd, Y$). The resulting solutions if filtered with a $0.2 \mu\text{m}$ hydrophilic syringe filter, can be purified with a size-exclusion chromatography column (Sephadex LH20). Gold, gadolinium, and yttrium concentrations in solution can be determined by ICP-MS analysis. For illustration, in parallel, different dilutions of the Gd-DtNP solution ($[Gd]$ from 201 to $34 \mu\text{M}$) are shown as they were analyzed, and a mean Au/Gd-ratio of 3.6 was measured. The Gd-DtNP solutions using scanning transmission electron microscopy coupled to energy dispersive X-ray analysis (STEM-EDX; see Figure S2 in the SI) showed size distributions from Feret's diameters (Figure 1, black

histogram) of particles obtained from TEM images (Figure S1 in the SI) and dynamic light scattering (DLS; Figure 1, red histogram).

4 ILLUSTRATION OF THIOL DERIVATIVE: DTDTPA-GADOLINIUM 13

TEM distribution from a deposit of particles on a carbon-coated copper grid while in DLS distribution is hydrodynamic diameter in solution. The distribution from DLS is narrower, but the overall result is good. From the distributions, a mean particle diameter of 4.8 nm obtained by microscopic picture of functionalized gold NPs using partially optimized molecular mechanics with the MM3 force field on Scigrass Explorer 7.7 program. A discrete sequence of truncated octahedral morphological motifs for gold NPs over 1.5 nm was a recent evidence. The particle formed was therefore described by the formula $\text{Au}_{201}[\text{Y-Dt}(\text{H}_2\text{O})_2]_{56}$ (Figure 2). The Au/Y ratio used was 3.6, corresponding to the mean Au/Gd ratio determined by ICP-MS.

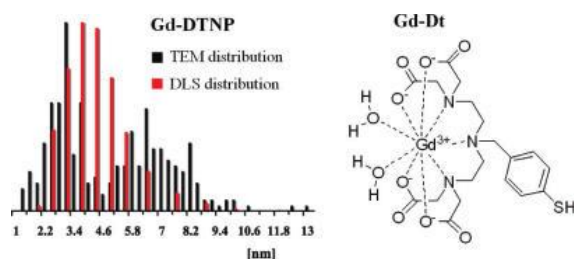


Figure 1. (left) Diameter size distributions obtained from (black) TEM images and (red) DLS. (right) Chelating unit Dt complexed with gadolinium (Gd-Dt).

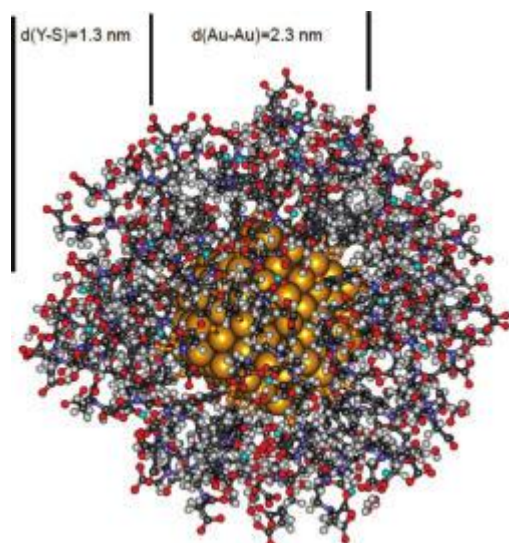


Figure 2. Partially optimized structure (MM3 force field) of Y-DtNP containing 201 gold atoms, 56 Y-Dt chelates, and 112 water molecules.

Visual inspection of a space-filling model (see Figure S4 in the SI) shows that the spherical shell formed by the Y-Dt chelates is densely packed. From the simple model, it can be deduced that the thickness of the spherical shell is 1.3 (0.3 nm, corresponding in this particular case roughly to the radius of the gold core). The total diameter of the modeled particle is ~ 4.9 nm and corresponds to the mean diameter of the Gd-DtNP measured by DLS. Thiol-covered gold nanoparticles are known to show magnetic behavior.¹¹ In view of the goal of creating particles that potentially can act as MRI contrast agents, any magnetic property of the particle is of natural interest. We determined the effective magnetic moment (μ_{eff}) per gadolinium ion in different dilutions of Gd-DtNP by ¹H NMR analysis using Evans' method.^{15,16} The μ_{eff} values of the solutions obtained from the experimental chemical shifts (Table S2 in the SI) are in close accordance with the effective magnetic moment of Gd^{3+} [$\mu_{\text{eff}}(\text{Gd}^{3+})$ 7.94]. No magnetic moment was detected from ¹H NMR shifts of the Y-DtNP solution, even at the high magnetic field of 18.8 T. The gold core of the NP therefore does not contribute significantly to the overall magnetic moment of Gd-DtNPs. The nuclear magnetic relaxation dispersion (NMRD) profiles of Gd-DtNP were measured at 25 °C (Figure 3). Both Gd-DtNP batches led to very similar relaxivities (r_1). A very high relaxivity maximum of ~ 60 mM⁻¹ s⁻¹ at 30 MHz was found, corresponding to a relaxation enhancement per NP of more than 3000 mM⁻¹ s⁻¹. Tillement⁶ and Kim⁷ both used ligands chelating several Gd^{3+} ions, leading to lower relaxivities but higher relaxation enhancements per NP.

Various theoretical approaches have been developed to analyze NMRD profiles of gadolinium compounds.¹⁷ We used the approach of Bertini et al.¹⁸ and Kruk et al.,¹⁹ which has been implemented in the software package developed in Florence and is called the "modified Florence method".²⁰ This method is well suited for fitting the experimental NMRD profiles for slowly rotating complexes of gadolinium(III), an $S = 7/2$ ion characterized by relatively low static zero-field splitting (ZFS). The data fitting was performed by fixing most of the parameters to values typical for Gd complexes with the DTTA chelating unit. The four parameters fitted were the overall rotational correlation time (τ_R 298), the correlation time for the transient ZFS (τ_v 298), and the amplitudes of the transient and static ZFS (Δt_2 and Δs_2 , respectively) (Table S3 in the SI). The results for the transient ZFS are close to the values found for the Ru-based metallostar $\{\text{Ru}[\text{Gd}2\text{bpy-DTTA}2(\text{H}_2\text{O})4]3\}4-$,²¹ which is built using the same chelating unit. However, the amplitude of the static ZFS is $\sim 30\%$ lower than that for $\{\text{Ru}[\text{Gd}2\text{bpy-DTTA}2(\text{H}_2\text{O})4]3\}4-$. A global rotational correlation time τ_R 298) 1.2 ns was calculated for Gd-DtNPs. The dense packing of the Gd-Dt units on the surface of the NPs makes them very rigid. The absence of internal rotation of the Gd-chelating units leads to a very good fit, even at high NMR frequencies (ν g 200 MHz).

5 APPLICATION OF DTDTPA-Gd50 IN MRI

MRI experiments on rats and mice were also carried out since the *in vitro* studies demonstrated the ability of AuDTDTPA-Gd to greatly enhance the MR images' contrast (Figure 7). The paper gives clear indication that these particles can be applied as contrast agents for MRI. A striking positive contrast appears first in the kidneys and then in the bladder. For illustration, MRI of the circulating particles injected in rats and in mice yielded identical results with X-ray imaging techniques in terms of size morphometry of tissue. Although the gadolinium content in AuDTDTPA-Gd is weaker than the gold content (5 mM versus 50.7 mM), the contrast induced by these particles is while kidneys are no longer observed by SRCT. Indeed MRI is more sensitive than X-ray imaging techniques, but it does not rule out the application of these particles as contrast agents for SRCT. If their use as positive contrast agents for clinical diagnosis by MRI should afford more reliable results, the SRCT which rests on the contrast generated by AuDTDTPA-Gd could be a key element for radiotherapy. Besides their ability to enhance the image contrast, AuDTDTPA-Gd could be applied as a radiosensitizer for radiotherapy using injection of gold nanoparticles (with a diameter of 1.9 nm but with an unknown surface composition) to tumor bearing mice led to the eradication of tumors after the mice were submitted to a X-ray beam whose dose is largely lower than the one delivered in the absence of gold particles. The SRCT, which is performed with the same X-ray beam as that for the therapy, would allow imaging of diseased tissue just before irradiation. As Au-DTDTPA-Gd50 nanoparticles permit us to visualize zones as small as the ureter (Figure 6), SRCT images will be done in order to determine that there is a sufficient amount of gold nanoparticles and to determine with high precision the zone to be irradiated. Such an application requires a selective targeting of the diseased tissue which can be accomplished through the grafting of cRGD in the case of solid cancerous tumors.

6 FUTURISTIC GOALS

There is indication that X-ray imaging and MRI experiments coupled to ICP analysis of Au-DTDTPA-Gd nanoparticles can be applied as liver, and spleen biotargeting. Specific targeting may be an art for the early detection of cancer and its treatment can be monitored by the covalent grafting of biotargeting groups on the organic multilayer of the Au-DTDTPA-Gd nanoparticles based on DTDTPA ligand 3COOH moieties as anchoring sites. Gold nanostructures induce the destruction of cancerous cells after activation with an external physical stimulus (electromagnetic radiation in X-ray and near-infrared spectral domains, the development of nanoparticles for targeted diagnosis and therapy can therefore be envisaged with Au-DTDTPA-Gd nanoparticles. New developments are expected in gold particles in NIR-PAI, OCT, US imaging.

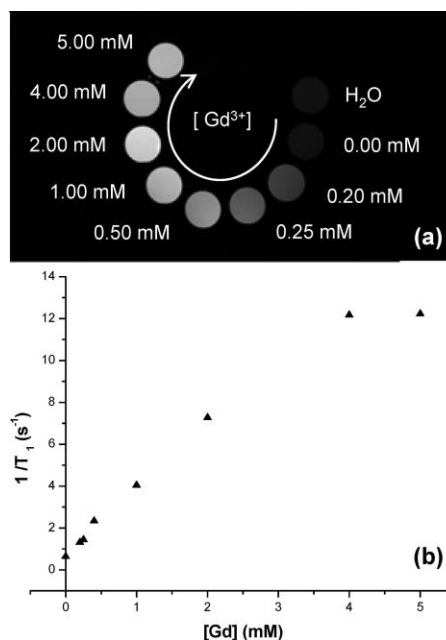


Figure 3. (a) T1-weighted magnetic resonance images of water as negative control (H₂O) and of aqueous colloids of Au-DTDTPA-Gd_x with increasing amount of Gd (from 0 (x) 0) to 5.00 mM (x ≈ 50 per particle, [Au]) 50.7 mM). (b) Water proton longitudinal relaxation rate (1/T₁) of Au-DTDTPA-Gd_x as a function of increasing gadolinium concentration.[1].

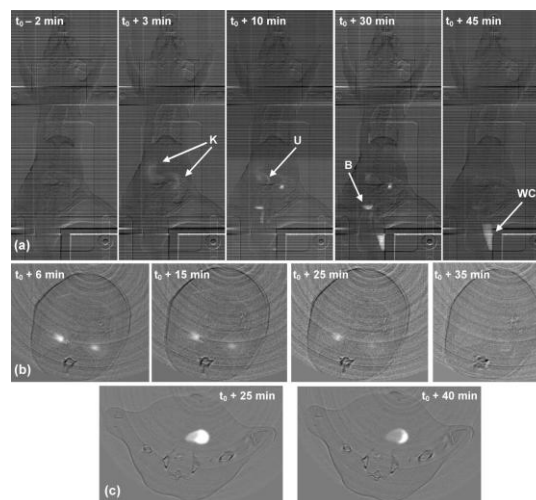


Figure 4. (a) Planar X-ray images in transmission mode of a rat before ($t_0 - 2$ min) and after injection of Au-DTDTPA-Gd₅₀ (K for kidneys, U for ureter, B for bladder and WC for the tube collecting the urine). SRCT images of transverse slices recorded at various times after injection of Au-DTDTPA-Gd₅₀ to a rat including (b) kidneys and (c) bladder (slice thickness: 1 mm).[1].

Some lead examples of gold particles in imaging are: 1. NIR contrast of cortical blood vessels in the *in vivo* rat brain cortical blood vessels; 2. feasibility in optical coherence tomography; 3. feasibility of using nanoshells *in vivo* as an NIR contrast agent in Reflection-mode PAI in molecular differentiation and highly sensitive and selective detection of skin cancers;

antibody conjugated gold nanorods as a molecular-specific contrast agent to improve the sensitivity of PAI for imaging in vivo inflammatory responses using bioconjugated gold nanorods with adhesion molecules, stimulated endothelial cells labeled with bioconjugated gold nanorods.

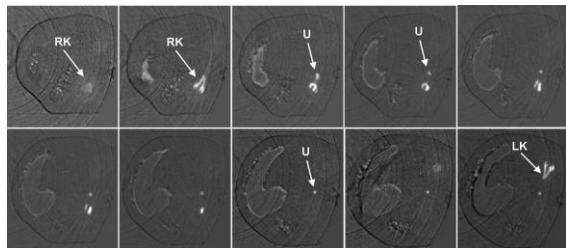


Figure 5. SRCT images of a series of successive transverse slices including right kidney (RK) of a rat from the head (top left) to the tail (right down). The images were recorded 10 min after the intravenous injection of Au-DTDTPA-Gd₅₀ to a rat (RK and LK for right and left kidneys, respectively; U for ureter).[1].

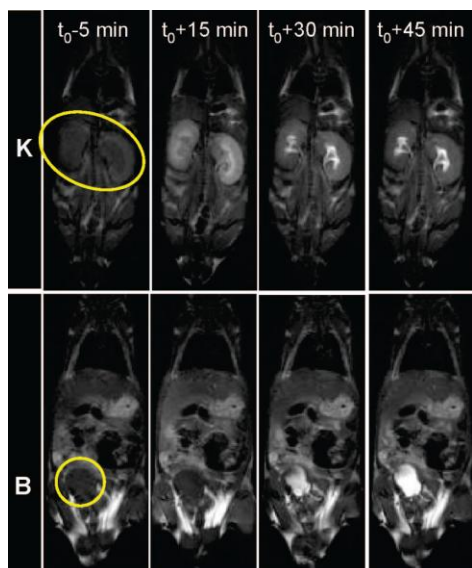


Figure 6. T1-weighted images of a mouse 5 min before (t₀-5 min) and 15, 30, and 45 min after intravenous injection of Au DTDTPA-Gd₅₀ (K for kidneys and B for bladder).

7 CONCLUSION

In conclusion, possibility of a small, stable, water-dispersible, DTTA thiol-functionalized gold NPs complexed with paramagnetic gadolinium or diamagnetic yttrium rare-earth ions is shown as multimodal imaging contrast agent. Characterizations using TEM images, DLS, and STEM-EDX analysis indicated a particle size distribution from 1 to 13 nm. Bulk magnetic susceptibility measurements at high magnetic field showed the absence of a significant magnetic contribution from the gold core. CT-MRI hybrid imaging techniques are progressing to save

imaging time. Gold nanocomposites have a good chance be an option of multimodal imaging contrast agents in hybrid imaging. PEBBLES represent a versatile platform for PAI in NIR region for deep tissue imaging, ligand targeting contrast agents to visualize molecular distribution by multifunctionalities.

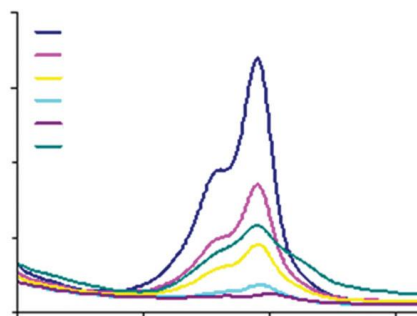
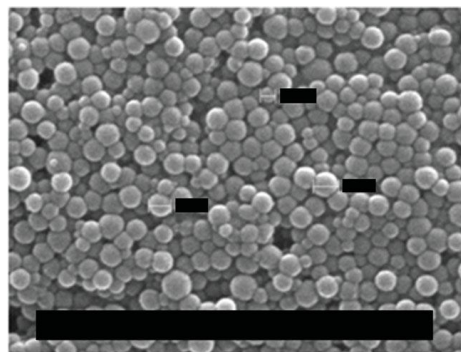


Figure 7: SEM image of ICG PEBBLE (a) and optical absorption of ICG PEBBLES and ICG free dye at different concentrations (b). Comparison yields a mean loading of 23000 ICG molecules per nanoparticles [2]

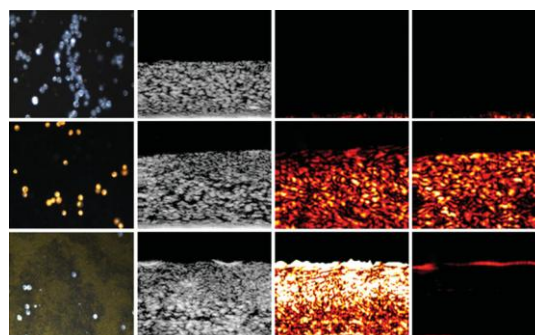


Figure 8: Darkfield, ultrasound and optoacoustic images ($\lambda = 532$ nm and 680 nm) of control, targeted and non-targeted tissue phantoms. The darkfield images measure $440 \mu\text{m}$ by $340 \mu\text{m}$ field of view. The ultrasound and optoacoustic images measure 2 mm by 1.67 mm.[3].

3 REFERENCES

1. *J. Am. Chem. Soc.*, **2008**, *130* (18), pp 5908–5915.
2. *J Biomed Opt* 2007, 12: 044020: 1-8.
3. *Opt Express* 2007, 15:6583.